D-Meson Production in 800-GeV/*c* *pp* Interactions

R. Ammar,[1] R. C. Ball,[2] S. Banerjee,[3] P. C. Bhat,[4] P. Bosetti,[5] C. Bromberg,[6] G. E. Canough,[7] T. Coffin,[2] T. O. Dershem,[2] R. L. Dixon,[8] H. C. Fenker,[8] S. N. Ganguli,[3] U. Gensch,[9] P. Girtler,[14] A. T. Goshaw,[4] F. Grard,[10] A. Gurtu,[3] C. Hamilton,[11] V. P. Henri,[10] J. J. Hernandez,[12],[a] J. Hrubec,[1] M. Iori,[12],[b] L. W. Jones,[2] D. Kuhn,[14] D. Knauss,[9] I. D. Leedom,[11] P. Legros,[10] J. Lemonne,[13] H. Leutz,[12] X. Liu,[1] P. K. Malhotra,[3] J. M. Marraffino,[15] G. E. Mendez,[4] R. Miller,[6] T. Naumann,[9] A. Nguyen,[6] H. Nowak,[9] P. Pilette,[10] J. Poirier,[7] A. Poppleton,[12] R. Raghavan,[3] K. Rasner,[14] S. Reucroft,[11] W. J. Robertson,[4] B. P. Roe,[2] A. Roth,[5] M. Senko,[15] W. Struczinski,[5] A. Subramanian,[3] M. C. Touboul,[12],[c] B. Vonck,[13] L. Voyvodic,[8] J. W. Waters,[15] M. F. Weber,[2] M. S. Webster,[15] and C. Zabounidis[11]

(LEBC-MPS Collaboration)

[1]*University of Kansas, Lawrence, Kansas 66045*
[2]*University of Michigan, Ann Arbor, Michigan 48109*
[3]*Tata Institute of Fundamental Research, Bombay 400005, India*
[4]*Duke University, Durham, North Carolina 27706*
[5]*III. Physikalisches Institut der Technischen Hochschule, D-5100 Aachen, Federal Republich of Germany*
[6]*Michigan State University, East Lansing, Michigan 48824*
[7]*University of Notre Dame, South Band, Indiana 46556*
[8]*Fermilab, Batavia, Illinois 60510*
[9]*Institut fur Hochenergiephysik, DDR-1615 Berlin-Zeuthen, German Democratic Republic*
[10]*Universite de l'Etat a Mons, B-7000 Mons, Belgium*
[11]*Northeastern University, Boston, Massachusetts 02115*
[12]*CERN, CH-1211 Geneva, Switzerland*
[13]*Inter-University Institute for High Energies, B-1050 Brussels, Belgium*
[14]*University of Innsbruck, A-60220 Innsbruck, Austria*
[15]*Vanderbilt University, Nashville, Tennessee 37235*
(Received 1 August 1988)

We report on a study of the inclusive production properties of $D/\bar{D}$ mesons in pp collisions at 800 GeV/c and compare our results to measurements made at lower energies and to the expectations of the QCD fusion model.

PACS numbers: 13.85.Ni, 14.40.Jz

Charm particle production in hadronic collisions has proven to be a useful test of the QCD parton-fusion model.[1] The model predicts an increase of the charm production cross section by about a factor of 3 between $\sqrt{s} \approx 26$–27 GeV and $\sqrt{s} \approx 53$–63 GeV while comparison of CERN-Super Proton Synchrotron (SPS) fixed-target experiments and CERN-Intersecting Storage Ring (ISR) experiments indicates a cross-section increase of at least a factor of 10.[2] Mechanisms other than the fusion model were invoked to explain this large increase in the charm cross section.[3] Recently this experiment, a study of charm production in pp reactions at 800 GeV/c ($\sqrt{s} = 38.8$ GeV) using the precision vertex detector LEBC (Lexan bubble chamber) filled with liquid hydrogen followed by a multiparticle spectrometer (Fermilab MPS), has reported a cross section consistent with an energy dependence for charm production in agreement with fusion-model predictions.[4] Those results used the topological uniqueness of charm decays, as seen in a hydrogen target and detector, to identify the data sample and thus involved only the LEBC data. Here we report on our measurements of the D meson x_F and $p_\perp$ behavior as determined from both the LEBC and the spectrometer data and compare them to the predictions of the fusion model.

We note that, in the absence of a well accepted procedure for correcting the nuclear effects, hydrogen target data taken with this chamber are the most reliable source of information on inclusive charm particle production in pp collisions.

The data were obtained during the third fixed-target running period of the Fermilab Tevatron accelerator. The LEBC-MPS apparatus was exposed to 800-GeV/c protons in the MT beam line. LEBC served both as a liquid-hydrogen target and as a high-resolution vertex detector upstream of the MPS. The chamber was operated so as to produce bubbles of 20 μm diam and a bubble density of 80 cm^{-1}. Two high-resolution proportional wire chambers positioned immediately downstream of the LEBC generated an interaction trigger

when more than two particles were detected in coincidence with an interacting beam particle. This resulted in a camera flash recording two stereoscopic views of the interaction in the LEBC and the simultaneous readout of the MPS. The two camers used conventional optics and gave 1.1×-demagnified pictures on 50-mm film. The overall trigger efficiency for events with charged multiplicity $n_{ch} \geq 4$ is $(88 \pm 2)\%$; for pp interactions producing charm, this efficiency becomes $> 99\%$.[4] A total of 1180000 triggers were taken which yielded about 500000 pp interactions in hydrogen. The remaining triggers corresponded to the LEBC wall events. The sample reported here consists of about 60% of the total exposure.

Each LEBC picture was double scanned and the charm candidates were selected for measurement by physicists in a third scan. Secondary vertices were classified as Cn (charged decay), Vn (neutral decay), or Xn (unclear, compatible with decay), where n is the number of charged particles leaving the decay vertex. Charm candidates have $n = 1,3,5$ for charged decays and $n = 2,4,6$ for neutral decays. The events were measured on an ERASME machine at CERN and an ADAM & EVA machine at Mons. Point measurement accuracy is 2 μm. Two tracks can be resolved if their separation is at least 20 μm and the decay tracks can be disassociated from the primary vertex if their impact parameters are greater than 10 μm.

The $V2$ decay sample has a large strange particle background and only those found in conjunction with another charm candidate were selected for measurement. Table I gives a summary of all measured candidates and the effects upon them of the geometrical selection criteria (cuts) used to yield an uncontaminated charm sample.[4] After measurement, a sample of 5 $C5$, 10 $V4$, 46 $C3$, and 23 associated $V2$ nonstrange decays remain. A study of all possible sources of background has shown that this sample is essentially free from noncharm decays.

TABLE I. Summary of the topological charm sample used in the cross-section determination and the effects upon them of the selection criteria (cuts). The numbers given are of those decays removed by the corresponding cut. The cuts are defined as follows. Length cut: decaying particle track length greater than 1 mm. Angle cut: no more than one decay track with either space angle greater than 150 mrad. Maximum i.p. cut: maximum decay track impact parameter greater than 50 μm (100 μm) and less than 1 mm (2 mm) for $V4$ ($C3$). Minimum i.p. cut: minimum decay track impact parameter greater than 20 μm. Also given for the $V4$ and $C3$ samples are the topological branching ratios and Monte Carlo weights used in the cross-section calculations.

Topology	$V2$	$C3$	$V4$	$C5$
Total number of decays	32	91	16	9
Length cut	7	12	2	0
Angle cut	1	9	0	1
Maximum i.p. cut	1	10	1	2
Minimum i.p. cut	0	14	3	1
Total after cuts	23	46	10	5
Branching ratio	···	0.43	0.17	···
Average weight	···	2.1	3.2	···

The mean charged-particle multiplicity at the primary vertex for events containing charm is 11.9 ± 0.8. This number does not include the charged particles from the observed charm decay(s). Correcting this number for decays which occur too close to the primary vertex to resolve, we obtain a charged-particle multiplicity of 11.0 ± 0.9. This value is to be compared with the value 10.26 ± 0.15 found for the mean multiplicity of all events at this energy.[5] However, if the charged particles from the charm particle decays are added, this gives, on average, an additional 4.6 ± 0.6 tracks per event,[6] yielding a total mean charged-particle multiplicity of 15.6 ± 1.1 for charm events at $\sqrt{s} = 38.8$ GeV. It is worth noting that all these multiplicity counts include both forward and backward hemispheres.

The measurement of the longitudinal and transverse momentum of the $D/\bar{D}$ mesons is based upon momentum determination and particle identification provided by the MPS detector. The bubble chamber and spectrometer information were merged via our reconstruction software package. Included in this procedure was a visual inspection of graphical event displays in order to optimize the reconstruction of charm decay tracks. The MPS particle tracking system included wire chambers upstream and downstream of a magnet which imparted a 700-MeV/c transverse momentum kick to charged particles. The momentum error plotted as $\Delta p/p$ versus momentum p for a sample of reconstructed tracks gives the straight-line fit $\Delta p/p = (0.3 + 0.01p)\%$, with p in GeV/c. This yields, for example, a momentum error of 1.3% at 100 GeV/c. Particle identification information was provided by nitrogen- and helium-filled Cherenkov detectors which had thresholds for π, K, and p of 5.7, 20, and 38 GeV/c and 16.7, 58.8, and 116 GeV/c, respectively and a transition radiation detector which is sensitive to particles with $500 < \gamma < 2000$. Details of the particle tracking and particle identification characteristics will be given in a future publication. The mass resolution of the LEBC-MPS arrangement for the $\pi\pi$ effective mass gives, for a sample of K^0 decays, the K^0 mass at 498.9 ± 3.7 MeV/c.[2] This compares favorably with the currently accepted value of 497.72 MeV/c^2.[7]

It is important to note that while the charm events contain a few examples of Λ_c and D_s candidates, they are predominantly D and $\bar{D}$ decays. The inclusive D production cross section is calculated from the samples of $C3$ and $V4$ D decays along with their respective topological branching ratios. The formula we use for each topological decay mode is

$$\sigma(D) = N_{obs}(D) W_{MC} / S B \epsilon_s ,$$

where $\sigma(D)$ is the D cross section, N_{obs} is the number of observed D decays into the mode with branching ratio B, W_{MC} is a Monte Carlo computed visibility weight which corrects for scanning losses and the cuts described below, and S is the sensitivity of the data sample. For the subsample discussed in this Letter, $S=9.7\pm0.5$ events/μb. The scanning efficiency ϵ_s, computed from a comparison of the two independent scans, is 0.90 ± 0.05. The visibility cuts are applied, for each decay, to the following quantities: (a) the decaying particle track length; (b) the impact parameters of the decay tracks at the primary vertex; and (c) the space angles of the decay tracks at the decay vertex. These cuts were chosen to ensure that the overall detection probability is high, to suppress Λ_c and D_s decays and to minimize topological ambiguities. More details of the scanning and visibility criteria and of the visibility weight Monte Carlo technique are given elsewhere.[4]

A summary of the numbers of decays used in the cross-section determination, both before and after the cuts, and of the weights and branching ratios for each topology are given in Table I. The resulting $D/\bar{D}$ inclusive production cross sections, for all x_F, are

$$\sigma(D^+/D^-)=26\pm4\ \mu\text{b},$$

$$\sigma(D^0/\bar{D}^0)=22^{+9}_{-7}\ \mu\text{b},$$

and

$$\sigma(D/\bar{D})=48^{+10}_{-8}\ \mu\text{b}.$$

The errors quoted are due to statistical effects. The estimated systematic uncertainty in each case, due mainly to the branching ratio error, is 25%.[8]

Not all of the decays given in Table I can be used to investigate x_F and $p_\perp$ behavior since not all of them have an unambiguous kinetic fit giving a unique D momentum. A total of 31 decays do have acceptable kinematic fits and Fig. 1 shows the resulting x_F and $p_\perp^2$ distributions for this decay sample. All decays are corrected for bubble chamber visibility losses and spectrometer acceptance. The solid curves show the result of a maximum-likelihood fit to the empirical form:

$$(1-|x_F|)^n e^{-ap_\perp^2},$$

with $n=8.6\pm2.0$ and $a=0.8\pm0.2$ (GeV/c)$^{-2}$. The fit was over the range $0.0<x_F<1.0$, where our detection efficiency is well known (note that there are no decays with $x_F>0.5$). Taken together with results from lower-energy pp experiments at 360 GeV/c (Ref. 9) where $n=1.8\pm0.8$, $a=1.1\pm0.3$ (GeV/c)$^{-2}$, and at 400 GeV/c (Ref. 10) where $n=4.9\pm0.5$ and $a=1.05\pm0.10$ (GeV/c)$^{-2}$, we see a stable $p_\perp$ behavior while x_F distribution steepens as the energy increases.

The QCD fusion model can be used to estimate the hadronic production characteristics of D mesons. Published structural functions[11] are used to describe the parton makeup of the proton and an empirical parton transverse momentum distribution of the form[12]

$$dN/dk_\perp^2 \propto e^{-k_\perp^2/\langle k_\perp^2\rangle},$$

is imposed with $\langle k_\perp^2\rangle=0.64$ (GeV/c)^2. The latter accounts for both the intrinsic parton transverse momemtum and soft gluon effects. We use published subprocess cross sections[13] and use $2m_c$ for the $c\bar{c}$ production thresholds, where the effective charm quark mass m_c is 1.25 GeV/c^2. The strong-interaction coupling constant is given by $\alpha_s=(12\pi/25)\log(Q^2/\Lambda^2)$ with $\Lambda=0.2$ GeV. The Q^2 parameter is chosen to be the square of the total

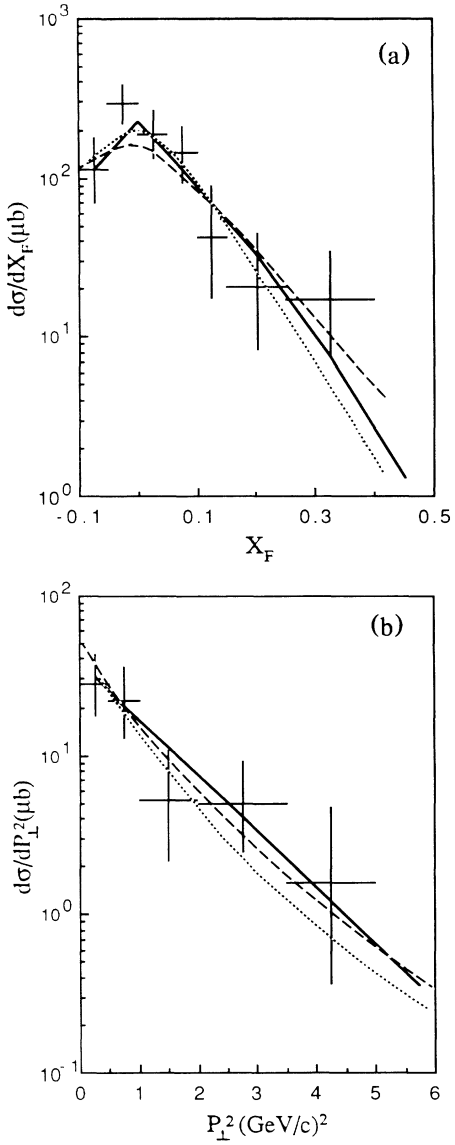

FIG. 1. (a) $d\sigma/dx_F$ and (b) $d\sigma/dp_\perp^2$ distributions for the kinematic fit $D/\bar{D}$ sample. The solid curves show the results of a fit to the data with an empirical form and the dotted and dashed curves show the results of fusion-model calculations. See text for details.

energy of the parton subprocess $\hat{s}$. For the $c \rightarrow D$ fragmentation process we have used the Lund model[14] with parameters determined from charm production in e^+e^- collisions. In order to evaluate the importance of the final-state fragmentation effects introduced by the Lund model, we have also calculated the D differential distributions assuming that the full c momentum is transferred to D (δ-function fragmentation).

Figure 1 compares the results of the fusion-model calculations, normalized to our data, to the measured x_F and $p_\perp^2$ distributions. The dashed curves are from the Lund fragmentation, the dotted curves show the result for a δ-function fragmentation. The Lund fragmentation process produces a somewhat flatter x_F distribution because of the quark effects in the D formation process. Both fragmentation choices give an adequate description of the data.

Summarizing, we have measured the characteristics of D meson hadroproduction in pp collisions at 800 GeV/c. The mean charged-particle multiplicity of events containing charm (excluding the charm decay products) is 11.0 ± 0.9. The total inclusive cross section is $\sigma(D/\bar{D}) = 48^{+10}_{-8}$ μb. The differential cross section is well represented by the form $d^2\sigma/dx_F dp_\perp^2 \propto (1 - |x_F|)^n e^{-ap_\perp^2}$ with $n = 8.6 \pm 2.0$ and $a = 0.8 \pm 0.2$ $(\mathrm{GeV}/c)^{-2}$ and is also in good agreement with the expectations of the QCD fusion model. We have compared our results with those of similar experiments at lower energy. The fusion model predicts that the production should become more central with increasing energy as more gluons at low x_F become sufficiently energetic to produce charm pairs. Our results are consistent with this prediction.

[a]Present address: Junta de Energia Nuclear, Madrid, Spain.

[b]Present address: University of Rome, Rome, Italy.

[c]Present address: University of Marseilles, Marseilles, France.

[1]R. K. Ellis and C. Quigg, FNAL Report No. FN-445, 1987 (to be published), and references cited therein.

[2]See, for example, S. Reucroft, in *Physics in Collision,* edited by M. Derrick (World Scientific, Singapore, 1987), and references cited therein.

[3]B. L. Combridge, in *Heavy Flavours,* edited by J. Tran Thanh Van (Edition Frontieres, Gif-sur-Yvette, 1982); S. J. Brodsky *et al.*, Phys. Rev. D **23**, 2745 (1981); R. C. Hwa, Phys. Rev. D **27**, 653 (1983).

[4]R. Ammar *et al.*, Phys. Lett. B **183**, 110 (1987).

[5]R. Ammar *et al.*, Phys. Lett. B **178**, 124 (1986).

[6]Extracted from D. Hitlin, Caltech Report No. CALT-68-1472, 1988 (to be published).

[7]M. Aguilar-Benitez *et al.*, Phys. Lett. **170B**, (1986).

[8]M. Aguilar-Benitez *et al.*, Z. Phys. C **36**, 551,559 (1987).

[9]M. Aguilar-Benitez *et al.*, Phys. Lett. **123B**, 103 (1983).

[10]M. Aguilar-Benitez *et al.*, Phys. Lett. B **189**, 476 (1987).

[11]Set 1 from E. Eichten *et al.*, Rev. Mod. Phys. **56**, 667 (1984).

[12]B. Cox and P. K. Malhotra, Phys. Rev. D **29**, 63 (1984).

[13]B. L. Combridge, Nucl. Phys. **B151**, 429 (1979).

[14]H. U. Bengtsson, private communication; H. U. Bengtsson and C. Ingelman, Comput. Phys. Commun. **34**, 231 (1985).